**Proceedings of the ASME 2019 International Design Engineering Technical Conferences & Computers and Information in Engineering Conference**
**IDETC/CIE 2019**
**August 18-21, 2019, Anaheim, CA, USA**

**IDETC2019-98112**

# MULTIBODY SIMULATION OF AN ELECTRIC GO-KART: INFLUENCE OF POWER-TRAIN'S WEIGHT DISTRIBUTION ON DYNAMIC PERFORMANCE

**Jonathan Mikler**
Department of Mechanical Engineering
Universidad de los Andes
Bogota, Colombia
Email: j.mikler10@uniandes.edu.co

**Santiago Camacho**
Department of Mechanical Engineering
Universidad de los Andes
Bogota, Colombia
Email: s.camacho13@uniandes.edu.co

**Andrew Bradley**
Head of the Autonomous Driving Research Group
School of Engineering, Computing and Mathematics
Oxford Brookes University
Oxford, UK
Email: abradley@brookes.ac.uk

**Andres Gonzalez-Mancera***
Associate Professor
Department of Mechanical Engineering
Universidad de los Andes
Bogota, Colombia
Email: angonzal@uniandes.edu.co

## ABSTRACT

*A multibody model of an electric go-kart was developed in Msc-Adams Car software to simulate the vehicle's dynamic performance. In contrast to an ICE kart, its electric counterpart bares an extra weight load accounted for the batteries and other powertrain components. The model is inspired on a prototype vehicle developed at Universidad de los Andes. The prototype was built on top of an ICE frame where a PMAC motor, controller, battery pack and the subsequent powertrain components were installed. A petrol-based Go-kart weight distribution was defined as baseline and several variants of the electric adaptation with different weight distributions were constructed. The main objective of the model is to evaluate different configurations and identify the ones that can give performance advantages. Step steer simulations ran at 40 km/h (64 mph) were analyzed to assess the dynamic performance of the vehicle for different configuration of the battery bank placement.*

*For most iterations of powertrain location, considerable differences in dynamic response were obtained and the handling balance was identified as Understeer contrary to a priori thoughs. Understeer gradient, weight distribution for both axles, trajectory among other results of interest were observed in the simulations.The model allowed to showcase the effect of redistribution of weight on the dynamic behavior in this specific application. Among the main consequences lies the fact that battery distribution can affect the lifting of the internal rear tire and the detriment in turning effectiveness.*

## 1 Introduction

Since the inception of Go-Karting in the 50's, several experimental, analytic and computational methods have been developed to analyze and enhance dynamic performance. Go-karts are characterized by the absence of differential and suspension, which makes its dynamics significantly different from that of other four-wheeled vehicles. The absence of rear differential places much importance on other areas of the vehicle; some more studied than others. Aspects like frame stiffness have had relatively numerous studies [1], [2], [3], while steering geometry and effects of powertrain adaptation and distribution have been left

*Address all correspondence to this author.

aside.

As with many other ground vehicles, trends are starting to shift into including electric power-trains instead of petrol-based for go-karts. Although these electric power trains have certain advantages, such as high torque throughout the range of angular velocities, the higher weight of the batteries have a direct effect on the overall weight and load distribution of the vehicle. This aspect makes it important to study and analyze the effect of the increased weight and modified load distribution. In previous analysis done on the dynamic response of go-Kart models, the most studied parameters have been the frame stiffness and steering geometry and its effect on the dynamic performance of the vehicle. It was shown [4] that a stiffer structure yields an improved response. Other authors [2] indicate that a higher elastic modulus, delivers better response to the steering wheel input resulting in higher level of lateral acceleration that has to be sustained by the tires.

In recent decades, multibody dynamic simulations have seen an increasing role in the state of the art of automobile analysis. Models have been widely used [3, 5] to predict the dynamic performance of ground vehicles. However, the construction of these models is a monumental challenge in both reverse engineering and direct engineering. A high fidelity model implies complex mathematical modelling of all sub-systems of the vehicle, as well as an experimental validation of said models. The case of the NADSdyna model is recognized as a pioneer in the field [3]. These models work as mathematical representations of mechanical systems which are then solved by some *core solver* after the model has been developed by another piece of software typically called *pre-processor* [6].

As stated by different sources, despite kart dynamics being significantly different from other four-wheeled vehicles due to their lack of suspension [1] and offering a potential for developing new technologies [4], research around them is very much limited. Furthermore, as mentioned previously, most research revolves around influence of chassis stiffness on dynamic response. Therefore, it is of interest to explore other characteristic of Go-Karts which also impact their performance directly.

This work presents the study, through computer multibody dynamic simulation, of the effect of weight distribution on the performance of an electric go-kart. As stated above, electric go-karts are heavier than equivalent ICE karts due to the added weight of the batteries. Strategic placement of the battery cells may aid in mitigating the negative effect of the added weight in the vehicle dynamics. A typical petrol-based kart is modeled to serve as baseline and four different configuration for battery placement are evaluated. The model's topology and characteristics are presented in Sec. 2 as well as the main assumptions and compromises of the proposed model. In Sec. 3 the results are presented along with a general assessment of the model, analysis and recommendations.

## 2 Model development

**FIGURE 1**: E-KART PROTOTYPE

A model of an electric kart was developed in the *Msc-Adams/Car* software. The model includes the basic components for a multibody system. The model is based on a prototype being developed by the Department of Mechanical Engineering at Universidad de los Andes and shown in Fig. 1.

The prototype is based on a standard ICE kart frame, modified to host the components of the electric power train. The main components of this power train include a 48V battery pack (4 x 12V (4-Cell) 100Ah LiFeMnPO4) and a 6 Hp (15 Hp peak) PMAC electric motor and controller weighting in total approximately 38 Kg. The configuration of the battery pack, separated into four discrete battery banks (each 12V) offer the opportunity of exploring different configurations, each with different load distribution. As the batteries constitute the heaviest component, different configurations result in considerable different dynamic performance. Several configuration of the battery cells, leading to different weight distributions were realized and analyzed. The kart's dimensions and weights were measured to set a baseline to be used as reference for the Go-Kart modeling. Individual masses were placed in the final models as well as a 70 kg pilot. The dimensions of the wheels used in the Go-Kart, which are specific for competition, are 10 x 4.60 - 5 inches, and 11 x 7.10 - 5 for front and rear tires, respectively. The cornering stiffness value used was taken from the work by [4]. The principal parameters used for constructing the model are presented in Tab. 1.

The different model iterations for the electric version of the kart parted from a common structure shared by all variants, which encompassed the subsystems and their role as identified in Tab. 4, namely the body, the front and rear suspension, the front and rear tires and a steering system. It is assumed that the remaining, not modelled components (e.g. the two bars holding

**TABLE 1**: KART AND WHEELS SPECIFICATIONS

| Wheelbase [mm] | Front tack [mm] | Rear track [mm] | Mass [Kg] | $C_{\alpha 1}$ [deg/g] |
|---|---|---|---|---|
| 1040 | 870 | 1000 | 160 | 47.3 |
| Camber [°] | Caster [°] | Kingpin Axis [°] | CoG Height [mm] | $C_{\alpha 2}$ [deg/g] |
| 0.0 | 14 | 13 | 150 | 200 |
| Front radius [°] | Front radial stiffness [N/mm] | Rear radius [°] | Rear radial stiffness [N/mm] | |
| 124 | 150 | 130 | 200 | |

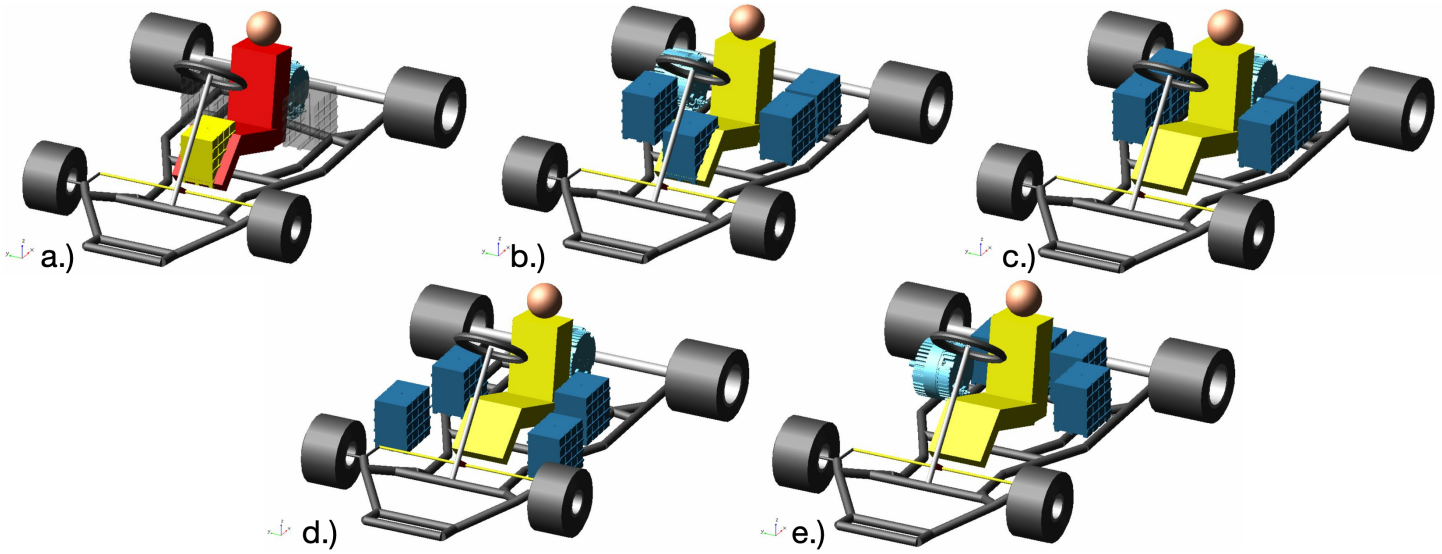


**FIGURE 2**: E-KART VARIANTS. a.) PETROL-BASED VARIANT, b.) E-KART VARIANT 1, c.) E-KART VARIANT 2, d.) E-KART VARIANT 3 AND e.) E-KART VARIANT 4

the steering shaft in its place for instance), have little effect on the overall dynamic response of the model. The entire chassis is assumed to be made of circular tubular sections of 32 mm of diameter with a thickness of 1 mm. Since it was easier to model the part as solid cylinders, the density of the part was adjusted so the weight of the part would match that one of the real chassis, which was already measured previously. The value for this density was $3.36 \times 10^{-6}$kg/mm3. Comparison with experimental measurements validated this approach.

For modelling the tire behavior, the properties for the *Pacejka* (Magic formula version 4 [6]) model was adapted, using most of the same parameters as the default *Msc-Adams/Car* version but adapting some parameters to fit reported data on kart tire behavior [4], since such detailed property data for competition Go-Kart tires are difficult to come by.

From an analytic point of view, the entire model would need to have ten degrees of freedom: the free movement of the Go-kart's body delivers six, the single degree of freedom from the steering system adds one more, each of the front wheels fixed at their respective hubs rotate around the left and right wheel-carrier meaning two more, finally, the rear axle rotates with it's wheels fixed to it around it's longitudinal axis providing the final degree of freedom.

Referring to the model joints in Tab. 2, joining the bodies together and restricting their movement are 16 joints and 1 reduction gear, which in turn impose 79 constraints. Additionally, an imposed motion is considered, given the selected maneuver (Step Steer). Gruebler's equation can be used to calculate the number of degrees of freedom:

**TABLE 2**: JOINT COUNT FOR THE ENTIRE MODEL

| Symbol | Element | Translational | Rotational | Total | N°of constrain elements |
|---|---|---|---|---|---|
| F | Fixed joint | 3 | 3 | 6 | 5 |
| R | Revolute joint | 3 | 2 | 5 | 7 |
| S | Spherical joint | 3 | 0 | 3 | 2 |
| H | Hooke joint | 3 | 1 | 4 | 2 |
| - | Motion (rotational) | 0 | 1 | 1 | 0 |
| Rg | Red. gear | 0 | 1 | 1 | 1 |

**TABLE 3**: Maneuver parameters

| Parameter | Value |
|---|---|
| Time | 5 s |
| Steps | 3000/s |
| Initial velocity | 40 / 60 km/h |
| Steering angle (right turn) | 15°(for 0.5 / 1 s) |
| Starting time | 1st sec. |

$$DOF = 6 \times (16-1) - 80 = 10 \quad (1)$$

### The Step Steer Maneuver

The Step Steer is a standard handling maneuver often used to evaluate handling response on vehicles [7] and was therefore selected for this work. The maneuver was performed applying at the steering shaft a right hand turn of 15°degrees[1] for different scenarios, namely at 40 and 60 km/h and 0.5 and 1 second turning time, this to avoid undesirable drifting. A convergence test was carried out to determine the minimum time step to assure convergence of the solution. A time step of 3000 steps/s was selected. The basic parameters of the maneuver are presented in Tab. 3. It should be noted that for the maneuver performed in this analysis, the simulation had an initial movement condition for the revolute joint at the steering wheel, thus eliminating one degree of freedom from the model.

Since the Go-Kart does not have a suspension system, the role of front suspension was given to a part-less subsystem, which only purpose is to communicate alignment parameters to the front wheels[2]. Similarly, the role of the rear suspension subsystem was given to the rear axle, performing the same job as the front suspension subsystem along with connecting the rear wheels to the rest of the vehicle. The detailed connection topology is presented in Fig. 3.

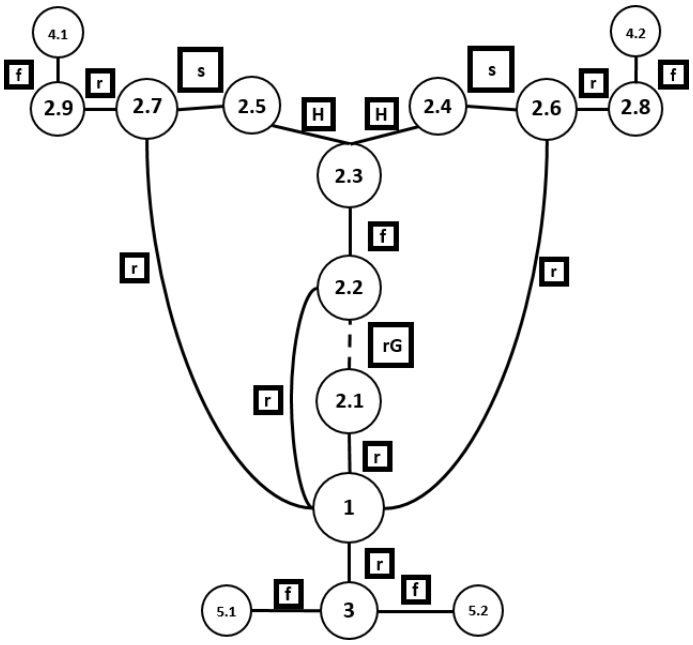


**FIGURE 3**: DETAILED TOPOLOGY OF THE MODEL

## 3 Results and Analysis

For the dynamic analysis, the behavior can be characterized using the understeer gradient, which expresses a direct relation of

[1]The maneuver is selected from a previously configured list of open-loop maneuvers, the direct motion configuration is done by *Msc-Adams/Car* internally

[2]*Msc-Adams/Car* demands the presence of six specific subsystems to develop a full vehicle assembly, one of such sub-systems is the front suspension

**TABLE 4**: MODEL'S PARTS AND ROLES

| Subsystem name | Part | Part ID | Role |
|---|---|---|---|
| Body | Chassis | 1 | Body |
| Steering | Steering wheel | 2.1 | Steering system |
| | Steering shaft | 2.2 | |
| | Lever Arm | 2.3 | |
| | Pitman Link [L] | 2.4 | |
| | Pitman Link [R] | 2.5 | |
| | Wheel carrier [L] | 2.6 | |
| | Wheel carrier [R] | 2.7 | |
| | Hub [L] | 2.8 | |
| | Hub [R] | 2.9 | |
| Rear Axle | Rear Axle | 3 | Rear suspension |
| Front tires | Front tire [L] | 4.1 | Front tires |
| | Front tire [R] | 4.2 | |
| Rear tires | Rear tire [L] | 4.1 | Rear tires |
| | Rear tire [R] | 4.2 | |

the vehicle's cornering response with its weight distribution and tire characteristics. From a theoretical standpoint, the understeer gradient is calculated using the tire cornering stiffness and the weight distribution [8]:

$$K = \frac{W_f}{C_{\alpha f}} - \frac{W_r}{C_{\alpha r}} \tag{2}$$

Where $C_{\alpha f}$ and $C_{\alpha r}$ are front and rear cornering stiffness, and $W_f$ and $W_r$ are the weight on the front and rear axles, respectively.

With the purpose of verifying the results of the simulation, an analytic approach for calculating the understeer gradient is in addition taken. The following equations represent the relation

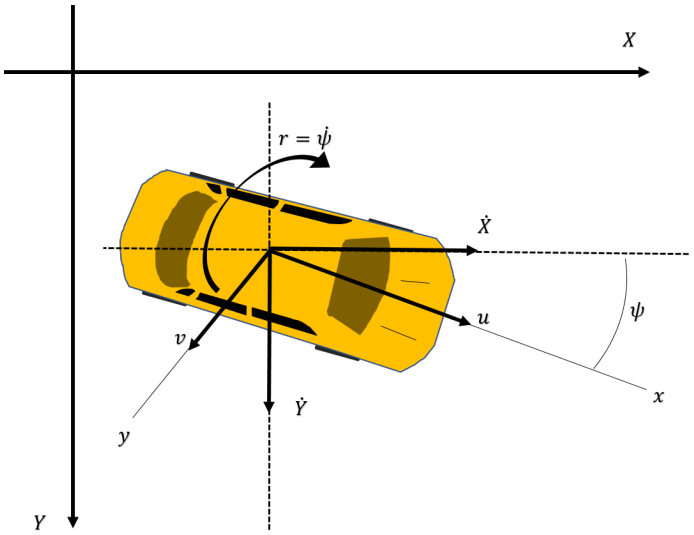


**FIGURE 4**: Vehicle Behavior for local and global coordinates

between the forces acting on the vehicle and its kinetic response for the $z$ and $y$ directions [9] which can shown in Fig. 4:

$$m\ddot{Y} = F_y \tag{3}$$
$$J_z\ddot{\psi} = M_z \tag{4}$$

where $\ddot{Y}$ is the lateral acceleration and $J_z$ is the polar moment of inertia in the $z$ direction. In turn, both equations 3 and 4 can be re-written as:

$$m(\dot{v} + ur) = F_{y1} + F_{y2} \tag{5}$$
$$J_z\dot{r} = aF_{y1} - bF_{y2} \tag{6}$$

Where $a$ and $b$ are the distances between the vehicle's center of gravity and the contact patch center in both the front and rear axles for a single-track depiction of the vehicle, $F_{y1}$ and $F_{y2}$ are front and rear axles lateral forces respectively and $u$ and $v$ are the centripetal and linear velocity of vehicle.

Under steady state conditions of turning, both the yaw acceleration and the lateral acceleration part which is not accounted for in the centripetal effect are cancelled, yielding the following equations:

$$mur = F_{y1} + F_{y2} \tag{7}$$
$$aF_{y1} = bF_{y2} \tag{8}$$

Shifting the focus on the normal forces $F_z$, the load are ob-

tained from equilibrium in the x-z plane:

$$F_{z1} = mg\frac{b}{L} \tag{9}$$

$$F_{z2} = mg\frac{a}{L} \tag{10}$$

By finding $a$ and $b$ in each equation, we obtain the following relation:

$$\frac{F_{y1}}{F_{z1}} = \frac{F_{y2}}{F_{z2}} \tag{11}$$

Given that the lateral forces $F_{y1}$ and $F_{y2}$ are dependant on the slip angle $\alpha$ the following is true:

$$\frac{F_{y1}(\alpha_1)}{F_{z1}} = \frac{F_{y2}(\alpha_2)}{F_{z2}} \tag{12}$$

Where $F_{y1}$ and $F_{y2}$ are front and rear axles normal forces.

Given the relation between the lateral force $F_y$ and the product of cornering stiffness $C_\alpha$ and slip angle $\alpha$ we can rewrite such equation as:

$$\frac{C_{\alpha1}\alpha_1}{F_{z1}} = \frac{C_{\alpha2}\alpha_2}{F_{z2}} \tag{13}$$

Additionally, replacing this equation into equation 7, the following relation is obtained:

$$\frac{u^2}{gr} = \frac{C_{\alpha1}\alpha_1}{F_{z1}} = \frac{C_{\alpha2}\alpha_2}{F_{z2}} \tag{14}$$

With $R$ being the radius of turn of the vehicle. Given the relation presented in equation 14, the following equation can be derived.

$$\alpha_1 - \alpha_2 = \left[\frac{F_{z1}}{C_{\alpha1}} - \frac{F_{z2}}{C_{\alpha2}}\right]\frac{u^2}{gr} \tag{15}$$

$$\alpha_1 - \alpha_2 = Ka_y \tag{16}$$

$$K = \frac{\alpha_1 - \alpha_2}{a_y} \tag{17}$$

This allows the computation of the understeer gradient $K$ by dividing the slip angles for some side of the vehicle by its lateral acceleration in g's.

Another way to characterize dynamic behavior is using the yaw rate, which is defined in the following equation:

$$r = 57.3\frac{u}{r} \tag{18}$$

A first approach to assess the sensitivity of the weight distribution is to evidence a typical dynamic phenomenon. Along the negotiation of a corner of a given radius, by virtue of lateral acceleration, a lateral weight transfer develops and is observable in the variation of normal forces at the wheels. Figures 5 show the redistribution of the weight during the maneuver. As shown in Fig. 5d, the rear internal wheel gets less unloaded in some configurations such as electric variant 4 and variant 2. This is important as the kart turning performance depends on this wheel getting fully unloaded and 'lifting' under certain conditions.

By contrast, variant 3 presents a better longitudinal weight distribution, which in turn yields a narrower cornering as seen in Fig. 6. Comparing this variant to the petrol-based case, it is observable that in spite of the additional weight, the performance is similar. Similarly, we observe in Fig. 7 that the angular velocity for both variant 3 and the petrol-based model are the highest values at turning, further strengthening the remark of variant three as a suited competitor for the petrol-based model.

As is typical in Go-Karts, the effect of the caster in loading the inner frontal tire is observed in all cases. However, as expected, a bigger load on the front would signify a higher chance on rear internal tire lifting. Such effect (front internal tire loading) is desired, as it enables a more effective turn by avoiding the *push forward* effect, this in turn a consequence of the absence of differential on the rear axle.

Understeer behavior was made evident in the trajectory followed by all vehicles, as seen in Fig. 6. In the figure, the turning radius, in spite of keeping the steering angle constant, increases with time. In terms of the specific understeer gradient however, as presented in Tab. 5 the calculated values differ from the theoretical values. In the simulations case, the best performing variants (Petrol and V3) have similar values, whereas the rest of the variant have a higher understeer characteristic. The difference between the theoretical and simulation-computed values is though to be accounted for three different causes, The weight distribution ratio, the dynamic behavior of the cornering stiffness and the uneven lateral weight distribution.

The weight distribution ratio on the theoretical calculations was held as 0.5, meaning that half of the total weight distribution to the outside is taken by the front wheel and half to the back. However, this might not be the case. Since there is no suspension system present, the proportion of the weight transfer that happens at the front and rear depend, for this model's case, on the differences on stiffness on the tires. Additionally, being that the construction and therefore the tire model parameters for the front and rear tires differ from one another, such stiffness is

**TABLE 5**: KART VARIANTS' THEORETICAL UNDER-STEER GRADIENT

| Parameters | Petrol | Electric V1 | Electric V2 | Electric V3 | Electric V4 |
|---|---|---|---|---|---|
| Weight [N] | 1307,8 | 1395,2 | 1395,2 | 1395,1 | 1395,2 |
| Front Axle to CoG [%] | 46% | 47% | 43% | 49% | 43% |
| Rear axle to CoG [%] | 54% | 53% | 57% | 51% | 57% |
| Left side to CoG [%] | 50.4% | 49.0% | 49.9% | 49.9% | 49.2% |
| Right side to CoG [%] | 49.6% | 51.0% | 50.1% | 50.1% | 50.8% |
| $K_{theory}$ [deg/g] | 9.19 | 10.17 | 8.71 | 10.89 | 8.71 |
| $K_{sim}$ [deg/g] | 6.44 | 7.03 | 7.60 | 6.56 | 7.84 |
| $r$ [deg/s] | 23.6 | 22.3 | 21.7 | 23.6 | 21.7 |

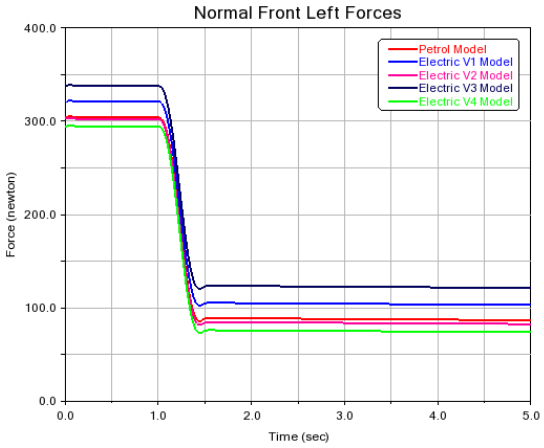


(a) Normal Forces: Front Left

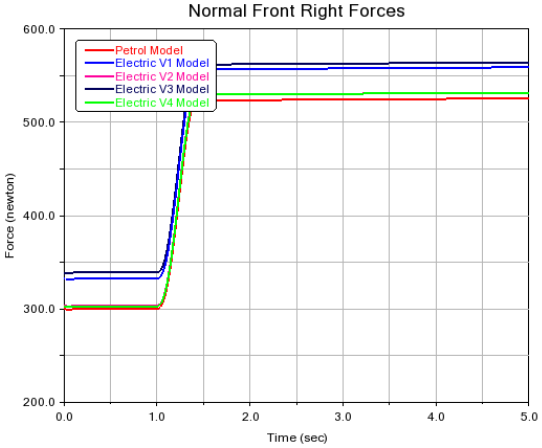


(b) Normal Forces: Front Right

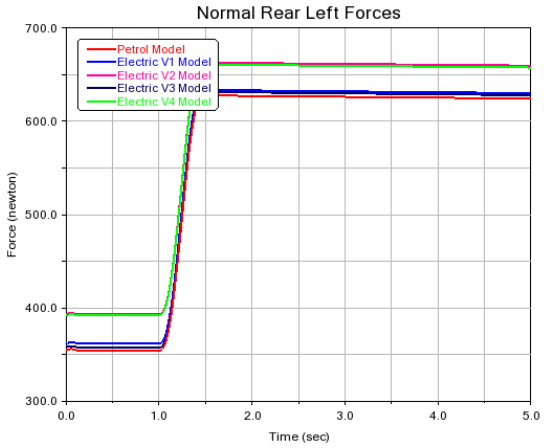


(c) Normal Forces: Rear Left

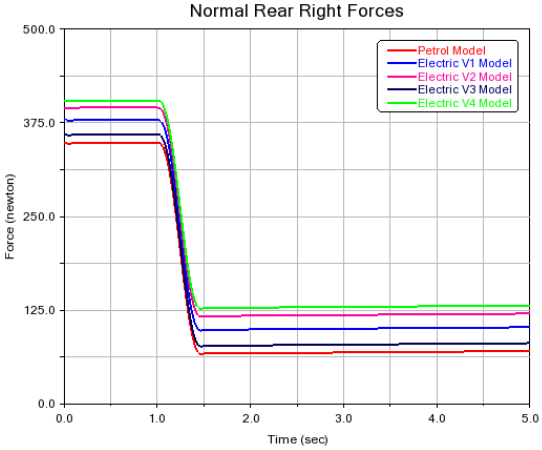


(d) Normal Forces: Rear Right

**FIGURE 5**: Normal Forces at 40 km/h

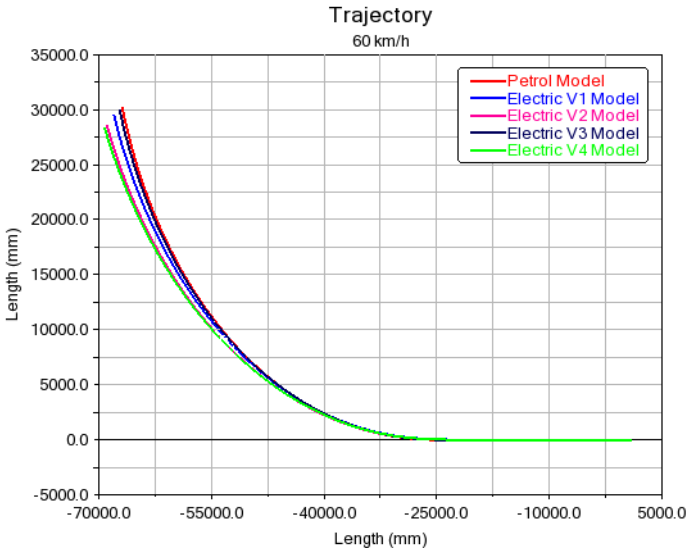


**FIGURE 6**: Simulation trajectory

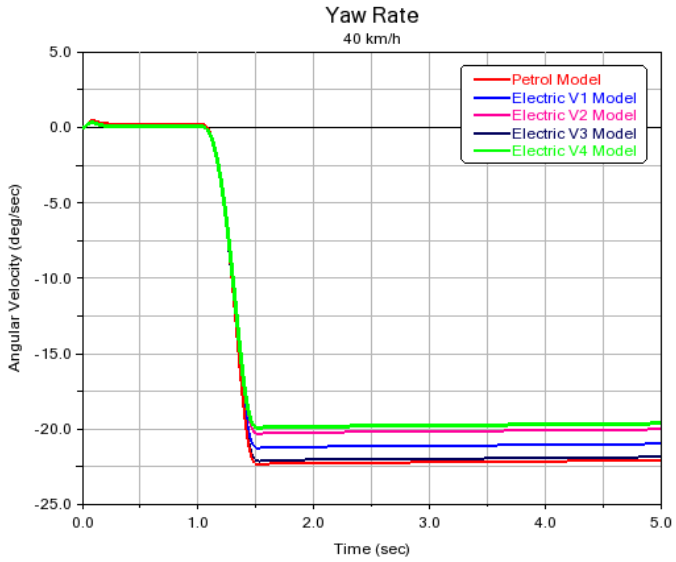


**FIGURE 7**: Yaw rates at 40 km/h for all variants

different (150 N/mm at the front and 200 N/mm at the back). All this would amount to the possibility that the front and rear tires carry different loads than initially though, offsetting the Understeer gradient value. Another key difference is that the Understeer Gradient computed from simulation results, is based on the Dynamic values of the slip angles and therefore, takes into account the Cornering Stiffness dynamic changes based (among other things) on the load variation. As the weight transfer manifests itself, the cornering stiffness reduces for the loaded wheels (outer ones) and reduces for the unloaded ones, such changes are not always symmetrical for the internal and external wheels and reduce the average value of the cornering stiffness. In cases were the rear axle is more loaded, the effect is higher, making the Understeer gradient vale decrease with respect to the computed Understeer Gradient value for static values of vertical load. This value is the one reported as theoretical value in table 5.

A less important effect, the lateral weight distribution (accounted for the a symmetry in the location of the batteries and the shift in position of the electric motor) makes the vertical load on all four wheels different, even if the weight transfer ratio was 0.5 and the cornering stiffness for all wheels where the same. In the electric variant 1 and 4, the motor is not located on the longitudinal axis but on one side, rendering it heavier and this, affecting the behavior for turning. This would not be taken into account in the theoretical value but indeed in the simulation-computed one.

Even though Understeer gradient does not coincide entirely between theory and simulation, yaw rate matches adequately. As seen in Tab. 5 yaw rate values are around 22 deg/s, the same showed by Fig. 7. For variant 3 and petrol-based model, theoretical yaw rate are the highest as it is expected base on previous analysis of dynamic performance. Similarly, Fig. 6 shows these models (V3 and petrol) taking a smaller corner radius than others variants, in the same way theoretical yaw rate suggested.

## 4 Conclusions

A multibody model of an electric Go-Kart was developed in the *Msc-Adams/Car* software, enabling the analysis of different configurations of powertrain location on the dynamic response of it. Given that a step steer portrays the transient response of the kart, the maneuver was selected for the steady-state cornering performance to be identified. The results suggest that the extra weight and its distribution affect the understeer coefficient, given that the handling of a kart is largely influenced by the need to lift the inner rear wheel due to the lack of a differential, and thus the addition of weight over the rear axle causes a tendency to understeer. Opposite to most competition vehicles' setups, a high oversteer condition is not desired in Go-Karts, therefore all setups of batteries though for competition must be ware of deviating too much from the neutral steer condition, where the inner wheel lifting might not occur.

Among the other configurations of distribution, one variant of the electric version, in spite of being about 15 kg heavier, presented a similar handling behavior than the petrol-based baseline, which comes in addition to the fact that the power output for electric motors gives a faster torque delivery, indicating that there is an argument on the similarity of competitiveness between ICE and electric sport Go-Karts. Additionally, and encompassing the suggestion of such variant, this paper has presented a methodology for the successful analysis, and improved understanding of the vehicle setup and handling characteristics when developing electric Go-Karts. This methodology should be aimed to define

an understeer gradient as small as possible countering tire stiffness on tires with a proper weight distribution.

The analysis also shows, that theoretical approach to characterize the cornering behavior in Go-Karts is more limited than in other four wheeled vehicles. This is partly because the discharge in the wheels leads to considerable changes in wheels cornering stiffness, rendering the initial value taken for the computing of Eqn. 2 somehow deviated from the actual value. In contrast, the calculation based on simulation results, Eqn. 17, presents a more accurate depiction of the understeer coefficient. For this, it is advisable to characterize such behavior through computational calculations. Moreover, both theoretical and computational values are positive, suggesting a necessity of positive correction in steer angle to follow a curve.

Improvements on the work should be done in different fronts. The characterization of the tires need further research to shape the parameters closer to the real wheel in elastic and viscous terms. Additionally, the elastic condition of the chassis was not taken into consideration, offsetting the entire result of the power source position.

## REFERENCES


[1] Lot, R., and Bianco, N. D., 2016. "Lap time optimisation of a racing go-kart". *Vehicle System Dynamics,* **54**(2), pp. 210–230.

[2] Muzzupappa, M., Matrangolo, G., and Gianpiero, V., Not Dated. "Methods for the evaluation of the go-kart vehicle dynamic performance by the integration of cad/cae techniques.".

[3] Pastorino, R., Sanjurio, E., Luaces, A., Naya, M. A., Desmet, W., and Cuadrado, J., 2015. "Validation of a real-time multibody model for an x-by-wire vehicle prototype through field testing". *Journal of Computational and Nonlinear Dynamics,* **10(3)**.

[4] Mirone, G., 2010. "Multibody elastic simulaton of a go-kart: correlation between frame stiffness and dynamic performance". *International Journal of Automotive Technology,* **11**(4), pp. 461–469.

[5] Heydinger, G. J., Salaani, M. K., Grygier, Garrott, W. R., and A., P., 2001. "Vehicle dynamics modelling for the national advanced driving simulator". *Journal of Automotive engineering,* **216**(Part D).

[6] Blundell, M., and Harty, D., 2014. *The multibody systems approach to vehicle dynamics*. Butterworth-Heinemann is an imprint of Elsevier.

[7] Allianz, F. T., 2018. Steady-state circular test. Accessed: 03-10-2018.

[8] Gillespie, T. D., 1994. *Fundamentals of vehicle dynamics*. Society of Automotive Engineers.

[9] Pavwelvssen, J. P., 2015. *Essentials of Vehicle Dynamics*. Butterworth-Heinemann.